Hindawi
Geofluids
Volume 2018, Article ID 6536419, 19 pages
https://doi.org/10.1155/2018/6536419

WILEY | Hindawi

Research Article

Feldspar Dissolution and Its Influence on Reservoirs: A Case Study of the Lower Triassic Baikouquan Formation in the Northwest Margin of the Junggar Basin, China

Meng Xiao,[1] **Xuanjun Yuan**,[1] **Dawei Cheng**,[1] **Songtao Wu**,[1] **Zhenglin Cao**,[1] **Yong Tang**,[2] **and Zongrui Xie**[2]

[1]*PetroChina Research Institute of Petroleum Exploration & Development, Beijing 100083, China*
[2]*Research Institute of Exploration and Development, Xinjiang Oilfield Company, PetroChina, Karamay, 834000 Xinjiang, China*

Correspondence should be addressed to Meng Xiao; xiaomeng422@126.com

Received 3 May 2018; Accepted 8 July 2018; Published 24 September 2018

Academic Editor: Tommaso Caloiero

Feldspar dissolution is a common feature in clastic rock reservoirs of petroliferous basins and has an important influence on reservoir quality. However, the effect of feldspar dissolution on reservoir quality varies under different depositional environments and diagenetic systems. The study area in this paper is located in the Baikouquan Formation in the northwestern margin of the Junggar Basin, which is significantly influenced by feldspar dissolution. Based on the analyses of core and thin section observations, QEMSEM, XRD, SEM, CL, fluorescence, and image analysis software combined with logging and physical property data, this study shows that feldspar dissolution in the subaqueous distributary channel of a fan delta plain, which has good original physical properties and low mud contents, significantly improves the properties of the reservoir. The main reasons for this are as follows: (1) the sedimentary facies with good original properties and low mud content is a relatively open system in the burial stage. The acidic fluids needed for feldspar dissolution are mostly derived from organic acids associated with the source rocks and migrate to the good-permeability area of the reservoir; (2) the by-products of feldspar dissolution, such as authigenic clay minerals and authigenic quartz, are transported by pore water in a relatively open diagenetic system and then precipitated in a relatively closed diagenetic system; and (3) the clay minerals produced by feldspar dissolution in different diagenetic environments and diagenetic stages have different effects on the reservoir. When the kaolinite content is less than 3%, the illite content is less than 4%, and the chlorite content is less than 12%, the clay minerals have a positive effect on the porosity. These clay minerals can reduce porosity and block pore throats when their contents are larger than these values.

1. Introduction

Approximately one-third of clastic rock oil and gas storage space is secondary porosity formed by mineral dissolution [1]. The migration process and precipitation of the by-products of mineral dissolution are important to the evolution of a reservoir [2–4]. Since the 1970s, there has been a large amount of research on the dissolution of single minerals by scholars. The organic acid dissolution theory was proposed, which covered topics such as organic acids produced by the thermal evolution of organic matter [5–7] and the dissolution mechanism of carbon dioxide from organic thermal evolution decarboxylation [8]. In addition, there is an atmospheric water dissolution mechanism [9, 10] and an alkaline fluid dissolution mechanism [11, 12].

Feldspar dissolution in clastic reservoirs is a common geological phenomenon that results in dissolution pores, which improve the physical properties of the reservoir [13–15], and also a popular research topic in oil and gas reservoir geology [2, 6, 16]. Temperature has significant effects on feldspar dissolution because as temperature increases, feldspar dissolution increases. However, the effect of pressure on feldspar dissolution is relatively weak [17]. When the environment changes from an acidic environment with low pH to an alkaline environment with high pH, the feldspar dissolution rate changes in the shape of a U. The dissolution

rate is slowest under neutral conditions [18]. The by-products of feldspar dissolution are mainly clay minerals and authigenic quartz [9]. Authigenic quartz is a common diagenetic mineral in the process of clastic rock diagenesis, with a formation temperature of 90°C [19] which is responsible for significant porosity and permeability reduction [20]. The formation of authigenic clay minerals, which is influenced by the geothermal and diagenetic fluid properties of the reservoir, affects the physical properties of the reservoir by introducing considerable micropores that impact the rugosity, saturation, and wetting characteristics [21, 22]. Smectite, illite, and chlorite mainly form under alkaline conditions, and kaolinite mainly forms under acidic conditions [23]. The conversion of smectite and kaolinite to illite mainly occurs between 70°C and 140°C. When the local temperature increases to 100°C–140°C, the illite-smectite mixed-layer clays convert to illite. If the concentrations of the iron and magnesium ions in the pore water are high, kaolinite can convert to chlorite under weak alkali conditions. As the pore flow velocity gradually increases, smectite converts to illite and chlorite [24].

Different scholars have different views on the influence of feldspar dissolution on a reservoir. Some scholars [25, 26] believe that grain particle dissolution, especially feldspar dissolution, can effectively improve the physical properties of the reservoir. However, other scholars [21, 27, 28] believe that with continuous feldspar dissolution, the ion concentrations in the pore water continuously increase. Precipitation occurs when the pore water reaches saturation and forms authigenic minerals, such as kaolinite, chlorite, illite, and authigenic quartz, which can occupy pore space, block throats, and thus reduce the quality of the reservoir properties. This saturation of the solution is related to temperature, pressure, flow velocity, and ionic species. The factors that control the effectiveness of reservoir dissolution in improving the physical properties of the reservoir are whether the diagenesis environment is open, the character of the fluid, the solubility of the minerals, and the geotemperature during diagenesis [15, 29].

The Baikouquan Formation in the Mahu Sag of the northwestern margin of the Junggar Basin is a typical conglomerate reservoir. Recently, continuous discoveries have been made and the proven reserves of the basin have reached 1.83 million tons, which indicates that the Baikouquan Formation is a good exploration prospect. In the study area, because of the high mud content and the poor original reservoir properties, feldspar dissolution is one of the key factors that determine the formation of high-quality reservoirs [30]. Therefore, this paper carries out a large number of core observations, intensive and representative sample collection, advanced research methods, and experimental means to analyse the influence of feldspar dissolution, its by-products on the reservoir, and provide a reliable basis for the future exploration of favourable reservoirs.

2. Geological Setting

The Junggar Basin is a large superimposed oil-gas basin in northwestern China with Late Carboniferous to Quaternary strata [31]. It can be further subdivided into six first-class tectonic zones [32]. It has characteristics of oil accumulation from multiple oil sources and multiple periods of hydrocarbon generation, accumulation, and adjustment in the oil-gas system [33]. Previous studies indicated that the Junggar Basin had a high geothermal gradient from the Carboniferous to Permian (the geothermal gradient has been estimated at 0.05°C/m–0.07°C/m), decreasing to 0.02°C/m–0.023°C/m in the Cenozoic [34]. The Mahu Sag, which is located in the northwestern Junggar Basin, is the most important hydrocarbon-generating sag in the basin [35]. The Mahu Sag is bounded to the northwest by the Wuxia and Kebai Fault Belts, to the east by the Shiyingtan Uplift, the Yingxi Sag, and the Sangequan and Xiayan Uplifts and to the south by the Dabasong and Zhongguai Uplifts [31] (Figure 1(a)). The Mahu Sag is a large depression lacustrine basin with an area approximately $6 \times 10^4\,km^2$ [36], and it mainly consists of a fan delta plain and fan delta front subfacies [37]. In the Late Permian, the Hercynian orogeny uplifted the northwestern basin and formed a series of high-angle thrust faults (Figure 1(b)). By the Triassic, the entire basin had evolved into an intracratonic basin, with sedimentation occurring on a stable basement. In the Late Triassic, the margins of the basin were still compressed [30]. The Baikouquan Formation is a gentle monocline structure that tilts to the southeast [38]. The strata in the slope area of the Mahu Sag are well developed, and the sediments that fill the basin comprise Carboniferous, Permian (Jiamuhe Formation, Fengcheng Formation, Xiazijie Formation, Lower Urho Formation, and Upper Urho Formation), Triassic (Baikouquan Formation, Kelamayi Formation, and Baijiantan Formation), Jurassic (Badaowan Formation, Sangonghe Formation, Xishanyao Formation, and Toutunhe Formation) and Cretaceous (Turpan Formation) deposits [31] (Figure 2). The Baikouquan Formation was deposited in the Triassic which unconformably overlies the Permian Formation (Figure 1(b)). It was deposited during the depression period of the tectonic evolution. During the whole burial process, the Baikouquan Formation existed in a warm, humid, fresh-brackish water, weakly oxidizing environment [39] and mainly consists of fan delta conglomerates, coarse sandstones, and some interbedded mudstones [38]. The Baikouquan Formation has a large accumulation of oil within multiple zones, but the conglomerate reservoir is tight and strongly heterogeneous (Kuang et al. 2005). Reservoir quality is considered the most important control on hydrocarbon accumulation in this area [40].

3. Samples and Methods

The conglomerate, sandstones, and clays analysed in this study are from the Upper Triassic Baikouquan Formation of the Xinjiang oil field, which is located in the northwestern margin of the Junggar Basin. Detailed core observation and logging analysis were conducted on 13 wells. We collected 283 samples from the 13 wells that consist of many types of lithology, lithofacies, and sedimentary facies. Of these 13 wells, three were selected for detailed sampling (Ma18, Aihu

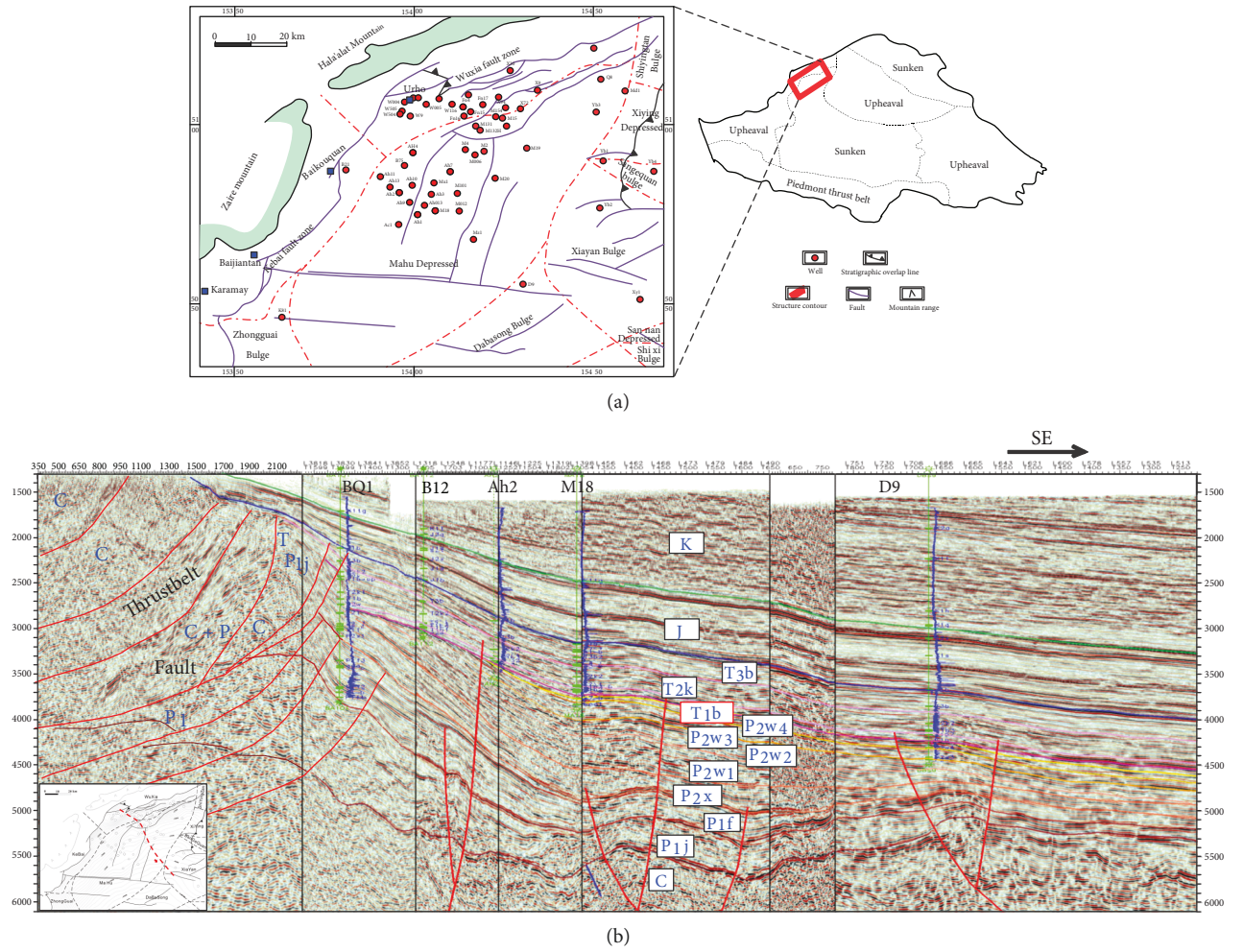

(a)

(b)

FIGURE 1: (a) Geological map of the western slope of the Mahu Sag in the northwestern Junggar Basin and (b) the south-east cross section showing the different tectonic structural zones and distribution of faults (seismic data are derived from the Research Institute of Exploration and Development, Xinjiang Oilfield Company).

1, and Ma003 wells), from which 97, 53, and 32 samples, respectively, were taken.

The rock composition data of 475 thin section samples (283 cast thin sections and 192 fluorescent thin sections), 8529 reservoir porosity and permeability data points, 622 grading analysis data points, 100 grain shape data points, and 275 mercury injection capillary pressure testing data points and logging data from 13 wells were obtained from the Research Institute of Petroleum Exploration & Development of the Xinjiang Oilfield Company, PetroChina.

More than 300 polished thin sections and 210 blue or red epoxy resin-impregnated thin sections were prepared for the analysis of rock composition, diagenesis, and visual pore characteristics. Because the grain size of the conglomerate is large, we made the thin sections 6 cm in diameter. The thin sections were partly stained with Alizarin Red S and K-ferricyanide for carbonate mineral identification. Point counting was performed on 30 thin sections, where at least 250 points were counted, with a deviation of approximately 6% [41]. A total of 65 reservoir conglomerate samples, 26 sandstone samples, and 3 interbedded mudstone samples were analysed for whole rock and clay fraction mineralogy using X-ray diffraction (the material that was larger than 2 mm was removed). For the contents of the carbonate cements, quartz cements, primary pores, and feldspar dissolution pores, 15 or 30 micrographs of 86 blue or red epoxy resin-impregnated thin sections were taken using a Zeiss Axioscope A1 APOL digital transmission microscope (for the coarse-grained conglomerates, 15 micrographs were taken; for the sandstones, 30 micrographs were taken). Then, the cements and pores in each micrograph were identified under the microscope and sketched on a computer using the CorelDraw software, and the total cement and pore contents in the 86 micrographs were obtained using the Image-Pro Plus software. Finally, the percentages of the cements and pores were calculated by taking the average of all values from the 15 or 30 micrographs. Cathode luminescence (CL) analyses were performed using an Olympus microscope equipped with a CL8200-MKS CL instrument. Twelve representative samples were viewed by a scanning electron microscope (SEM), and the major elements were analysed by using energy spectrum microanalysis. The SEM was equipped with an energy-dispersive X-ray spectrometer (EDX) using Quanta 450 FEG.

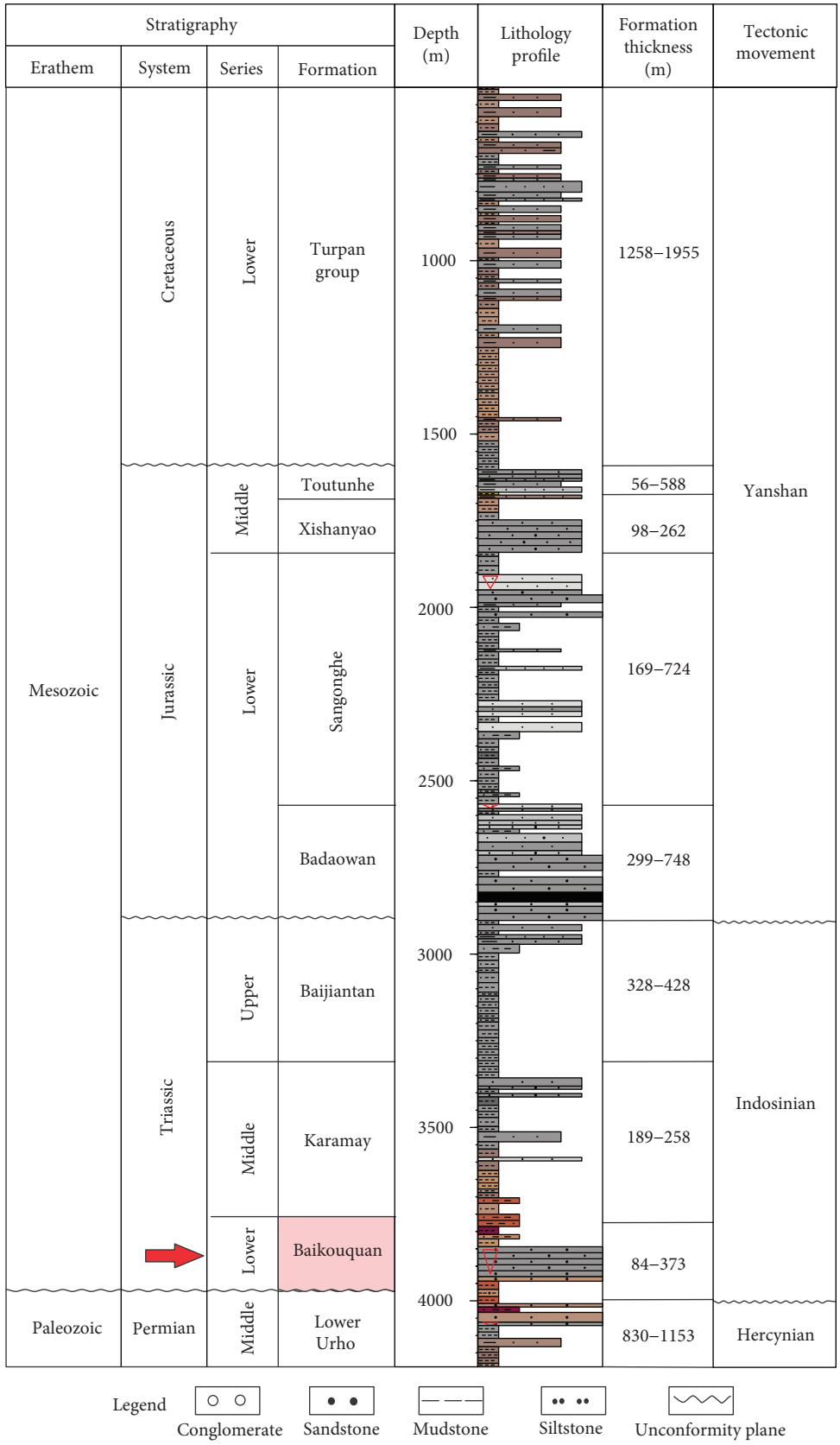

Figure 2: Lithostratigraphic columnar section of the western slope of the Mahu Sag in the northwestern Junggar Basin.

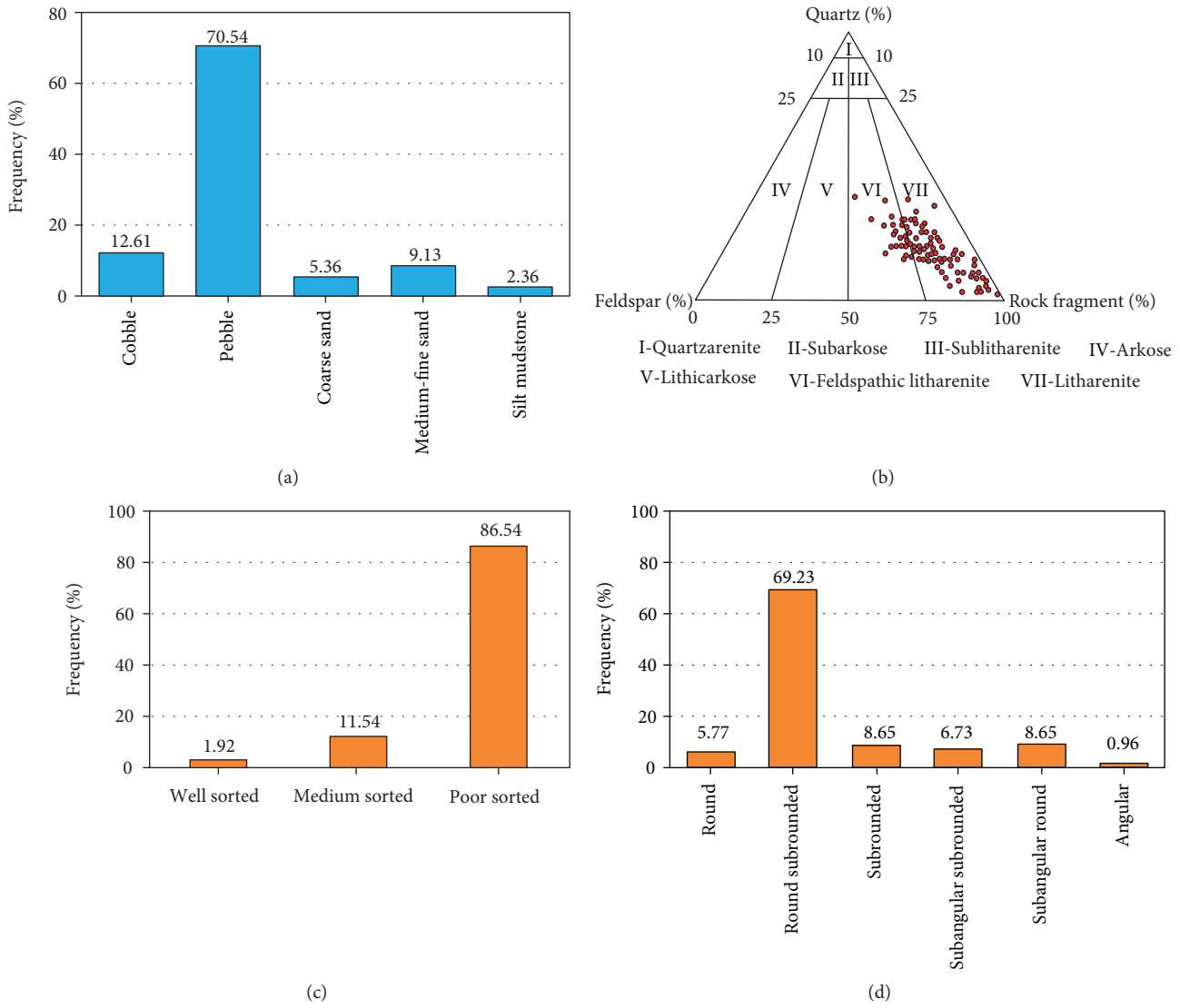

Figure 3: Lithological characteristics of the Baikouquan Formation. (a) Distribution characteristics of different types of lithology; (b) rock classification of the Baikouquan Formation; (c) sorting; (d) roundness. I: quartzarenite; II: subarkose; III: sublitharenite; IV: arkose; V: lithic arkose; VI: feldspathic litharenite; VII: litharenite.

To accurately analyse the mineral content of the sample and to quantify the percentage of the material around the mineral, 13 representative samples were cut into $0.5 \times 0.5 \times 0.3$ cm samples and their surfaces were polished. Using FEI Quanta 450 SEM, each sample was scanned continuously for 5×5 grid; then, the 25 fields were stitched into a complete image. Combined with QUEMSCAN analysis software, the mineral composition, pore size, and element data, as well as the composition of the material around the minerals, were determined.

4. Results

4.1. Detrital Composition of the Reservoir. The petrographic investigation of the Baikouquan conglomerate reservoir shows that the detrital components are mainly composed of conglomerates in which gravel accounts for 83.15% (boulders account for 1.21%, cobbles account for 11.4%, and pebbles account for 70.54%), sandstone accounts for 14.49% (5.36% coarse-grained sandstone and 9.13% medium- to fine-grained sandstone), and siltstone and mudstone account for 2.36% (Figure 3(a)). The XRD results show that the detrital components of the Baikouquan Formation comprise quartz (4.2–62.4%, average of 44.15%), feldspars (2.2–43.8%, average of 22.88%), and rock fragments (22.34–92.36%, average of 40.82%), indicating that the sandstones are mostly litharenite and feldspathic litharenites (Figure 3(b)). The grain size ranges from boulder to mudstone and is poorly sorted (86.54%) (Figure 3(c)). The grain shape is mainly rounded-subrounded (69.23%) (Figure 3(d)), which reflects a short distance to the sediment source.

4.2. Lithofacies. The Baikouquan Formation in Mahu Sag is a set of coarse-grained fan delta deposits and is mainly composed of conglomerate with complex lithology and high content of mud. A large number of studies have been done on

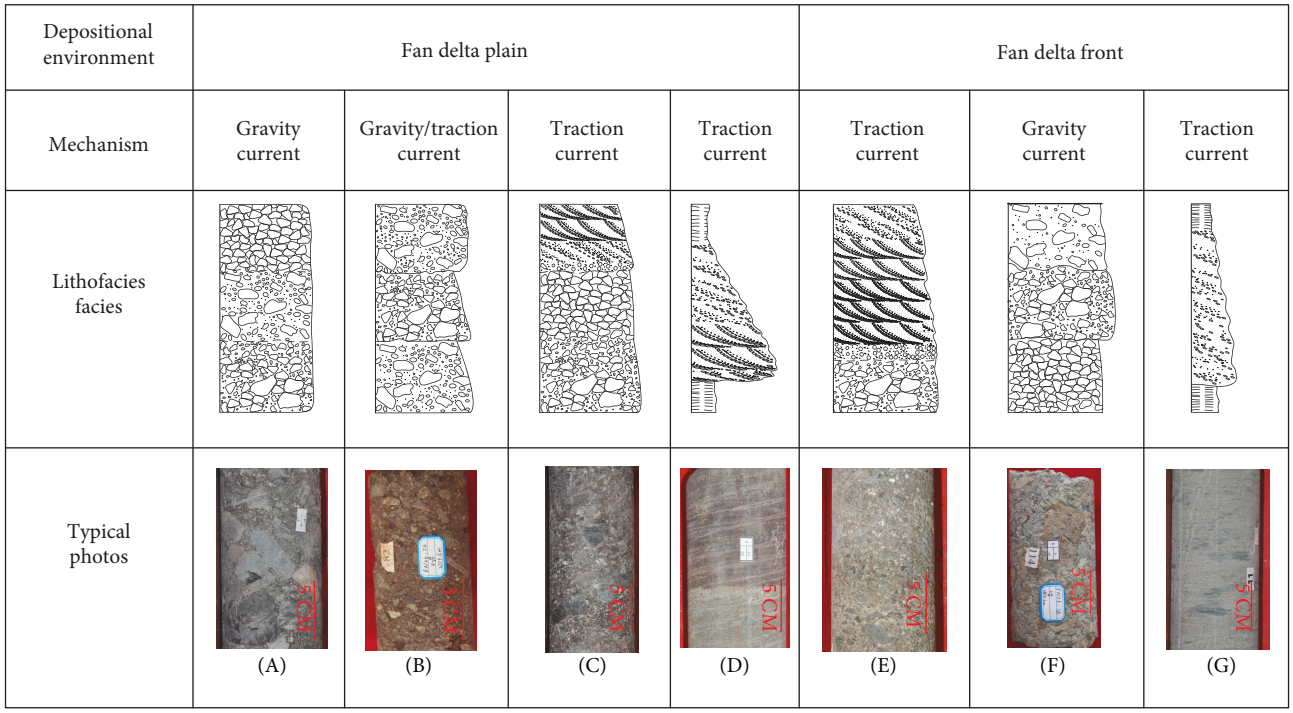

Figure 4: Different lithofacies characteristics of the Baikouquan Formation.

lithofacies [42, 43], and different classification of lithofacies has been made for different research purposes. Based on the formation mechanism, depositional environment, particle support type, cementation type, particle size, and colour, the sediment was divided into seven lithofacies (Figure 4) that represent the typical sedimentary characteristics in the study area: medium-grained to coarse-grained poorly sorted conglomerates that are mainly sand-gravel supported with angular grains and were deposited by gravity currents in the fan delta plain (Figure 4(a)); fine-grained to coarse-grained poorly sorted conglomerates that are mainly sandstone supported with angular grains and were deposited mainly by gravity and a little of traction currents in the channel with a temporary water flow (Figure 4(b)); coarse-grained sandstone to medium-grained conglomerates that were mainly deposited in the braided channel (Figure 4(c)); mudstone to medium-grained sandstones that were mainly deposited in the braided intrachannel (Figure 4(d)); fine-grained to coarse-grained moderately sorted sandstones, with generally subangular to subrounded grains and few clays, which were mainly deposited in the subaqueous channel of fan delta front (Figure 4(e)); fine-grained sandstone to coarse-grained conglomerates that are mainly multi-particle-supported conglomerates and were mainly deposited in debris flows (Figure 4(f)); and mudstone to siltstones that were mainly deposited in the subaqueous intrachannel (Figure 4(g)).

In the lithofacies (Figure 4(e)) with higher hydrodynamic of deposition and lower mud content, the porosity is larger and the connectivity is better, the pore size is generally larger than 100 microns, and the initial porosity and permeability are better than those of other lithofacies. In the diagenetic stage, it is easy to become an open diagenetic system due to the good fluidity of fluid; the lithofacies formed in the sedimentary environment with mainly gravity flow (Figures 4(a), 4(b), 4(c), and 4(f)) showed no obvious orientation and disorderly distribution of particles. With the high content of mud, poor separation, and grinding roundness, the dissolution pores of the reservoir are poorly developed and the pore size is generally less than 100 microns. The original physical property is poor. Because of the difficult migration of the fluid, with the dissolution and deposition of particles, a relatively closed diagenetic system is gradually formed.

4.3. Porosity and Permeability. A statistical analysis was performed on 1334 samples from the study area, resulting in a reservoir porosity distribution of 1.9%–16.8% (average of 8.54%); however, the porosity (Figure 5(a)) and permeability (Figure 5(b)) values of the P10 curves (where 10% of the reservoirs have higher values than these) show that some high values exist mainly in the coarse-grained sandstone and the granule stone. The P50 (median) curves show that some higher porosity and permeability intervals exist at 3840–3860 m and 3880–3930 m. The air permeability distribution of the reservoir is from 0.014 mD to 98.1 mD (average of 7.54 mD), and the main distribution range is 0.2 mD–1.0 mD. The percentages of the reservoir with air permeability values of less than 1 mD and 1–10 mD and greater than 10 mD are 44.19%, 37.06%, and 18.75%, respectively. The reservoir properties in the Baikouquan Formation are quite poor, and the heterogeneity of the reservoir is very high.

4.4. Pore Characteristics. Thin section and SEM observations revealed that the conglomerate reservoir pore types mainly consist of intraparticle dissolution pores (Figures 6(a), 6(d),

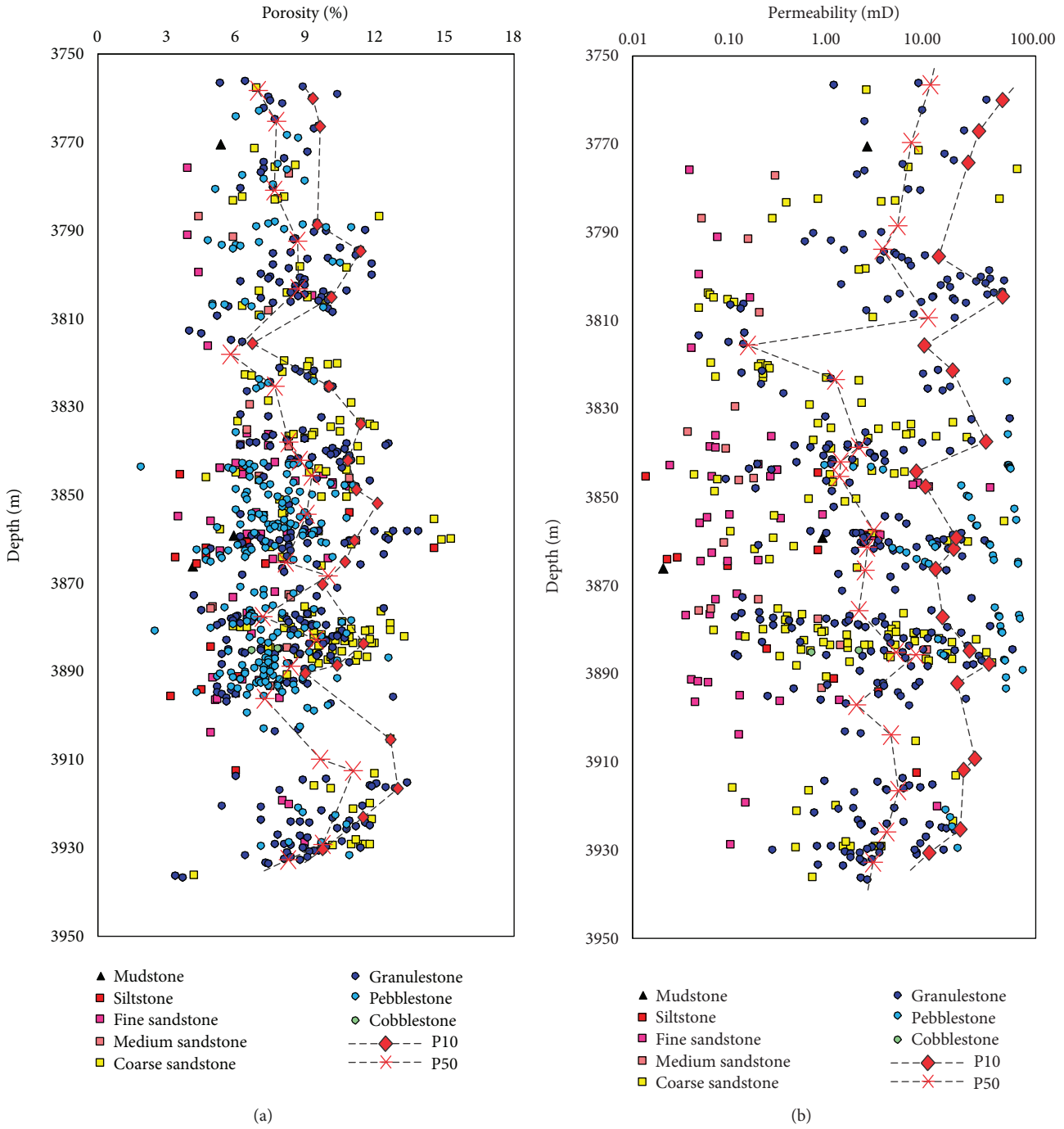

Figure 5: Relationship between physical property and depth in the Baikouquan Formation; (a) porosity; (b) permeability.

and 6(e)) and interparticle dissolution pores (Figures 6(a), 6(b), and 6(d)), with some mud shrinkage pores (Figure 6(f)). The interparticle dissolution pores (pore size > 100 μm) were mainly formed by alkali feldspar and acidic rock debris, and only a small amount was formed by calcite cement (Figure 6(c)). The intraparticle dissolution pores (pore size < 100 μm) were mostly produced by orthoclase dissolution. Residual interparticle pores are mainly present in the coarse-grained sandstones and granulestones, and they have better connectivity than the secondary pores. The proportion of intraparticle dissolution pores increases with increasing depth (Figure 7).

4.5. Feldspar Dissolution, Authigenic Clay Minerals, and Quartz Cement. The main diagenetic processes that control the reservoir evolution in the study area are compaction, dissolution, and cementation [44]. The paragenetic sequence includes compaction, early carbonate cementation, chlorite film, illite-smectite mixed-layer clays, feldspar dissolution, precipitation of kaolinite and quartz, montmorillonite

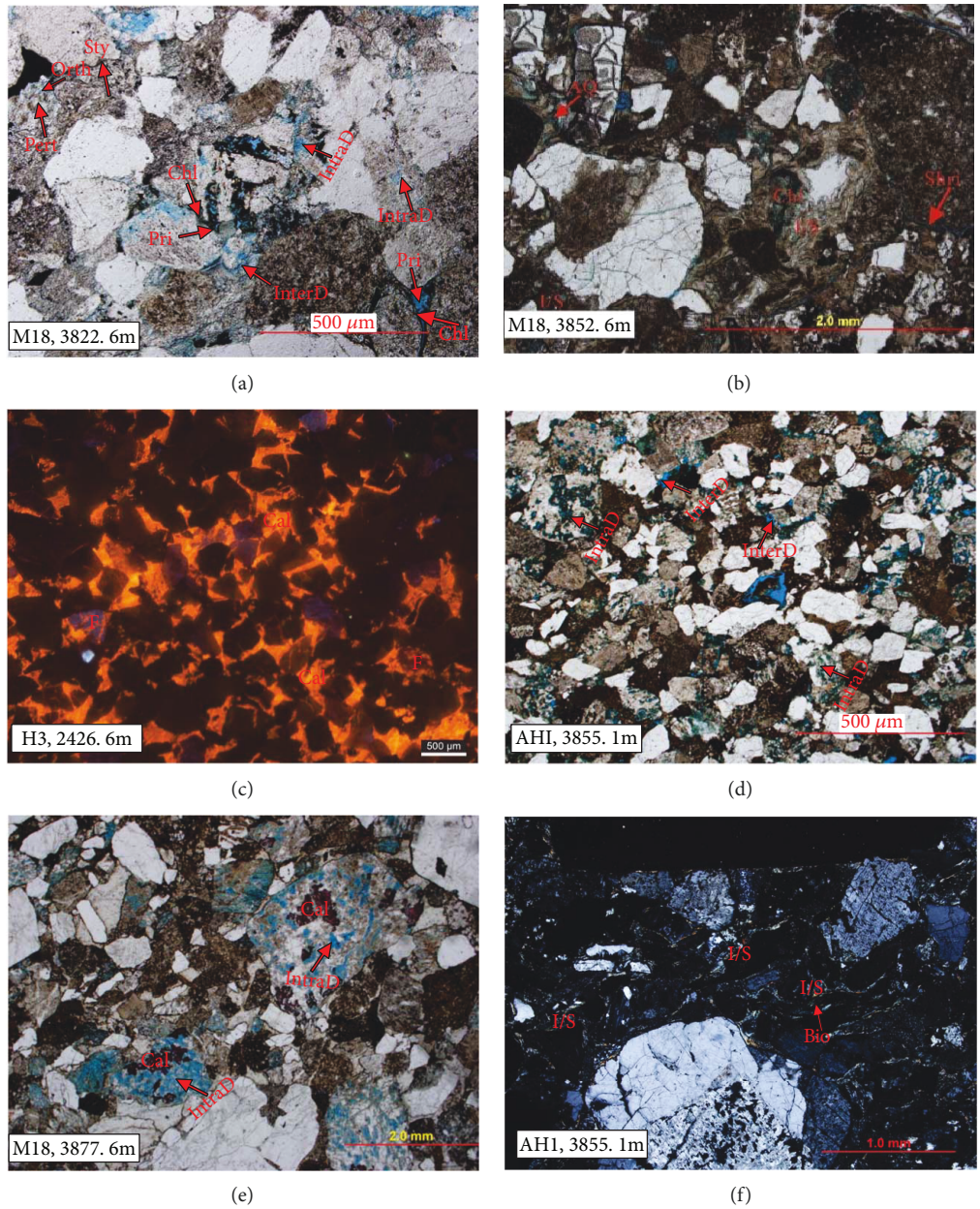

Figure 6: Thin section images of the Baikouquan Formation. (a) Plane-polarized light (PPL) images showing orthoclase dissolution with well-developed chlorite and well-preserved original pores; (b) PPL images showing that the intergranular pores are filled with illite in some reservoirs, and only a small amount of the pore is preserved; (c) cathodoluminescence images showing two phases of calcium cement filling the pores, and a small amount of the calcite is dissolved; (d): PPL images showing the developed dissolution pores in the tuffaceous rocks; (e) PPL images showing that calcite cementation is developed in the dissolution pores of the feldspars; and (f) cross-polarized images showing the illite-smectite mixed-layer clay filling pores in some reservoirs. Chl: chlorite film; Sty: stylolite; Pri: primary pore; Pert: perthite; Orth: orthoclase; I/S: illite-smectite mixed-layer clays; Shri: shrinkage; AQ: authigenic quartz; Cal: calcite cement; F: Feldspar; InterD: interparticle dissolution pores; IntraD: intraparticle dissolution pores; Tuff: tuffaceous; Diss: dissolution pores; K: kaolinite; I: illite.

illitization, and weak carbonate cementation [45]. In the study area, the microfracture is less developed which mainly formed at the edge of the gravel and the pore formed by grain dissolution is the main storage space in the reservoir. Feldspar dissolution pores account for the highest percentage of all the secondary pores [30]. The authigenic minerals mainly consist of carbonate cement (Figures 6(c) and 8(b)), kaolinite (Figures 8(a), 8(b), 9(b), 9(d), and 9(e)), chlorite (Figures 6(a), 8(a), 8(b), 9(a), 9(b), and 9(e)), illite (Figures 6(b), 6(f), 8(a), 8(b), 9(a), and 9(e)), illite-smectite mixed-layer clays (Figures 6(b) and 6(f)), and minor quartz cement (Figures 9(c) and 9(e)).

Feldspar grains that have a honeycomb-like texture in porous conglomerate reservoirs usually contain significant

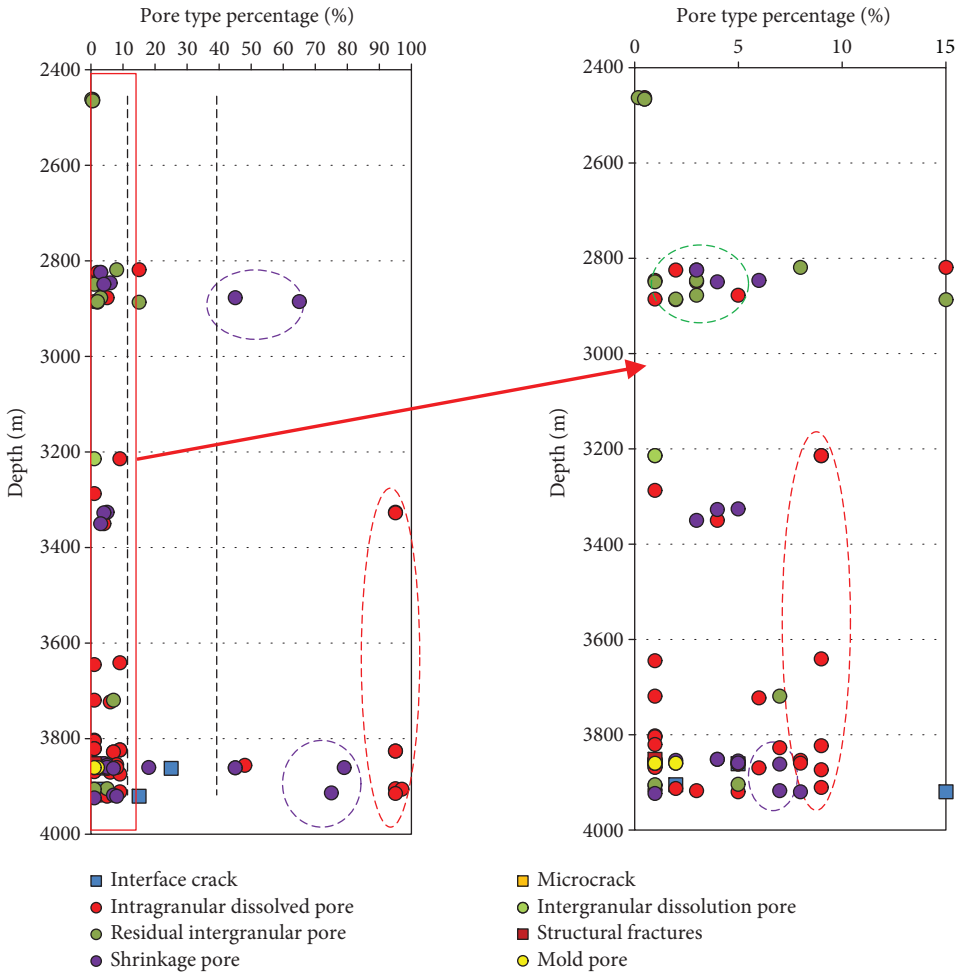

Figure 7: The relationship between the contents of pore types and depth.

dissolution pores (Figures 6(a), 8(a), 8(b), 9(a), 9(d), and 9(f)); these grains also display selective dissolution, where orthoclase is dissolved (Figures 8(b), 9(a), and 9(d)) but albite remains stable (Figure 8(a)) [30]. The quantitative porosity analysis of the thin sections shows that the porosity formed by feldspar dissolution can reach up to 6% and feldspar dissolution increases with increasing depth (Figure 10(a)). Quartz cements mainly occur in the form of quartz overgrowths (Figures 9(c) and 9(e)), with thicknesses ranging from 2 μm to 15 μm and a low content (less than 0.1%).

The XRD data and mineral analysis show that illite-smectite mixed-layer clays (average content is 16.61%) dominate the authigenic clays in the different reservoir samples, with minor chlorite (average content is 5.43%), illite (average content is 3.76%,) and kaolinite (average content is 2.33%). The SEM analysis revealed that kaolinite mainly occurs as vermicular aggregates and anhedral-pseudohexagonal plates (Figures 8(a), 9(b), 9(d), and 9(e)) filling the primary pores, illite-smectite mixed-layer mainly occurs in reticular form in the primary pores (Figures 6(b), 6(f), and 8(b)), chlorite mainly occurs around the particles (Figures 6(a) and 8(b)), and a few of the chlorite grains also fill the feldspar pores (Figure 8(a)). Some samples have a high content of illite-smectite mixed-layer clays of up to 78%, and the relative amount of kaolinite is less than 30%. The chlorite distribution is highly heterogeneous, with a maximum content of 64%.

According to XRD analysis, the residual amount of the feldspar in the study area is inversely proportional to the illite-smectite mixed-layer (Figure 10(b)) and is directly proportional to the kaolinite content (Figure 10(c)). With the continuous dissolution of the feldspar, the amount of residual feldspar decreases and a large number of kaolinite is formed in the early diagenetic stage. When the middle diagenetic stage is entered, the kaolinite gradually becomes into smectite and illite in an alkaline diagenetic environment. The pores and authigenic clay minerals formed by dissolution have a very important effect on the quality of reservoirs.

5. Discussion

5.1. Diagenetic Environment. Data from 74 pore water samples from conglomerate reservoirs show that 52.7% of these samples are characterized by $CaCl_2$ water, 43.2% are

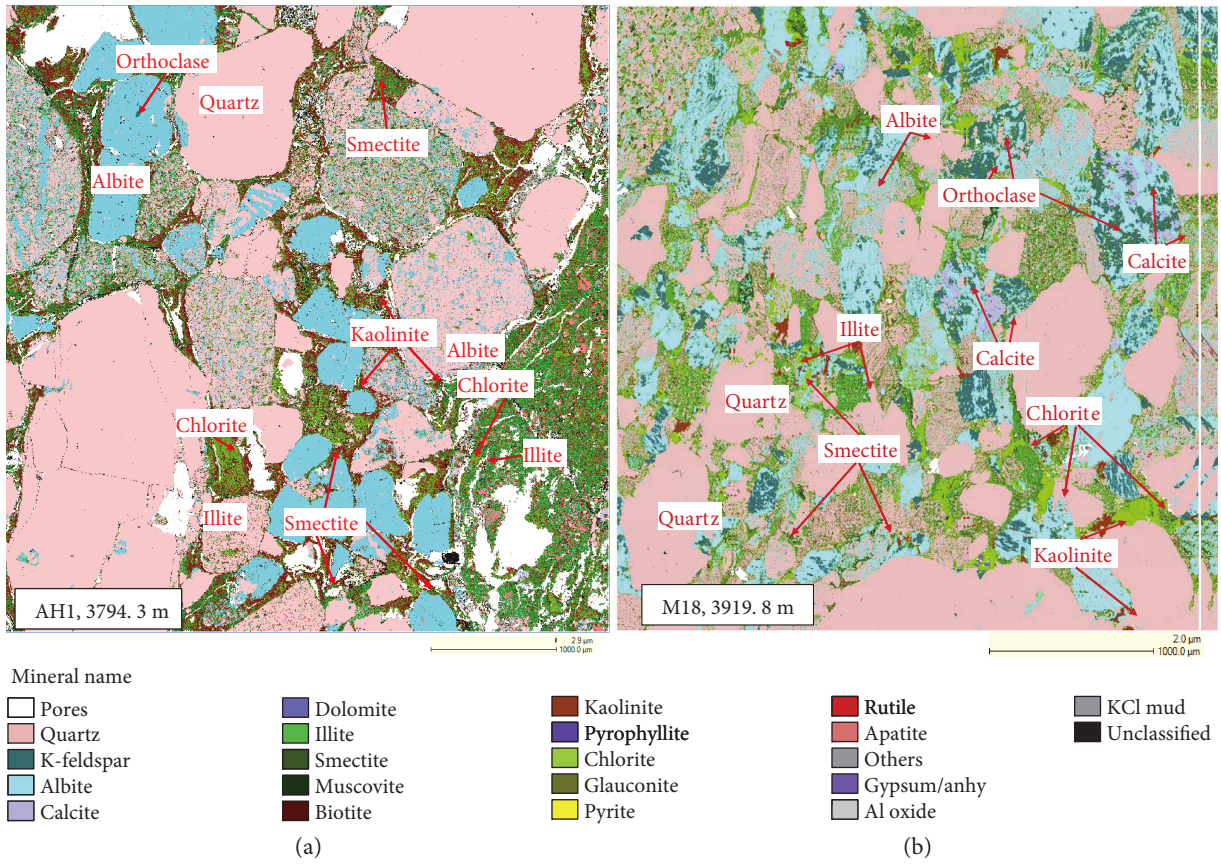

Figure 8: Mineral composition analysis of the Baikouquan Formation.

characterized by $NaHCO_3$ water, and 4.1% are characterized by $MgCl_2$ water. The salinity ranges from 2774.11 mg/L to 15,093.1 mg/L, which suggests that the pore water may come from different origins [46]. The subaqueous distributary channel (Figure 4(e)) mainly contains pebbles and coarse-grained sandstone which have lower salinity values than others and also has primary high porosity and permeability. The diagenetic environment in this sedimentary microfacies is relatively open (sample salinities are all lower than 7650 mg/L), the flow rate of the pore fluids is high, and the feldspar dissolution by-products are easily transported and rarely precipitated in situ (Figures 6(a), 6(d), and 6(e)). The sedimentary microfacies dominated by gravity flow (Figures 4(a), 4(b), 4(c), and 4(f)) with higher salinity value has a relatively closed system of diagenesis, and the acid dissolution strength of feldspar is low (Figures 6(b) and 6(f)). The data show that the salinity of the samples near the fault is relatively low (all lower than 6000 mg/L) and the fault can provide an effective channel for fluid migration, which highly impacts the feldspar dissolution. In addition, the organic acids generated by the source rocks of the Fengcheng Formation migrate along faults to reservoirs, which has an important effect on the feldspar dissolution [30].

5.2. Mineral Reactions and Mass Transfer. Feldspar dissolution in the study area mainly occurred in the mesodiagenetic stage [45]. The XRD results show that the albite content is higher (Figure 6(i)) (2.1%–35%) than the orthoclase content (0–4%). This result shows the selective dissolution of feldspar and indicates that orthoclase dissolution plays an important role in improving the physical properties of the reservoir [30]. Orthoclase dissolution increases with increasing depth. According to the statistical QUEMSCAN analysis, the minerals around the pores are mainly quartz (21.48%), albite (15.52), orthoclase (2.73%), chlorite (9.65%), and black mica (16.24%) (Figure 11(a)). The pores are mainly associated with feldspar dissolution. The minerals around the K-feldspar are mainly albite (35.48%), illite (28.24%), and quartz (14.82%) (Figure 11(b)). With continuous K-feldspar dissolution, the concentrations of by-products in the pore waters, such as those of Al^{3+} and SiO_2 (aq), exceed those needed for the saturation of kaolinite and quartz, as shown by the following equation [2, 13]:

$$KAlSi_3O_8 + H^+ + 0.5H_2O = 0.5Al_2Si_2O_5(OH)4 + 2SiO_2 + K^+, \quad (1)$$

where $KAlSi_3O_8$ is K-feldspar, $Al_2Si_2O_5(OH)_4$ is kaolinite, and SiO_2 is quartz.

The edges of the kaolinite mineral associations (Figure 11(c)) are mainly chlorite (30.97%) and illite (28.98%), indicating that part of the kaolinite converts to

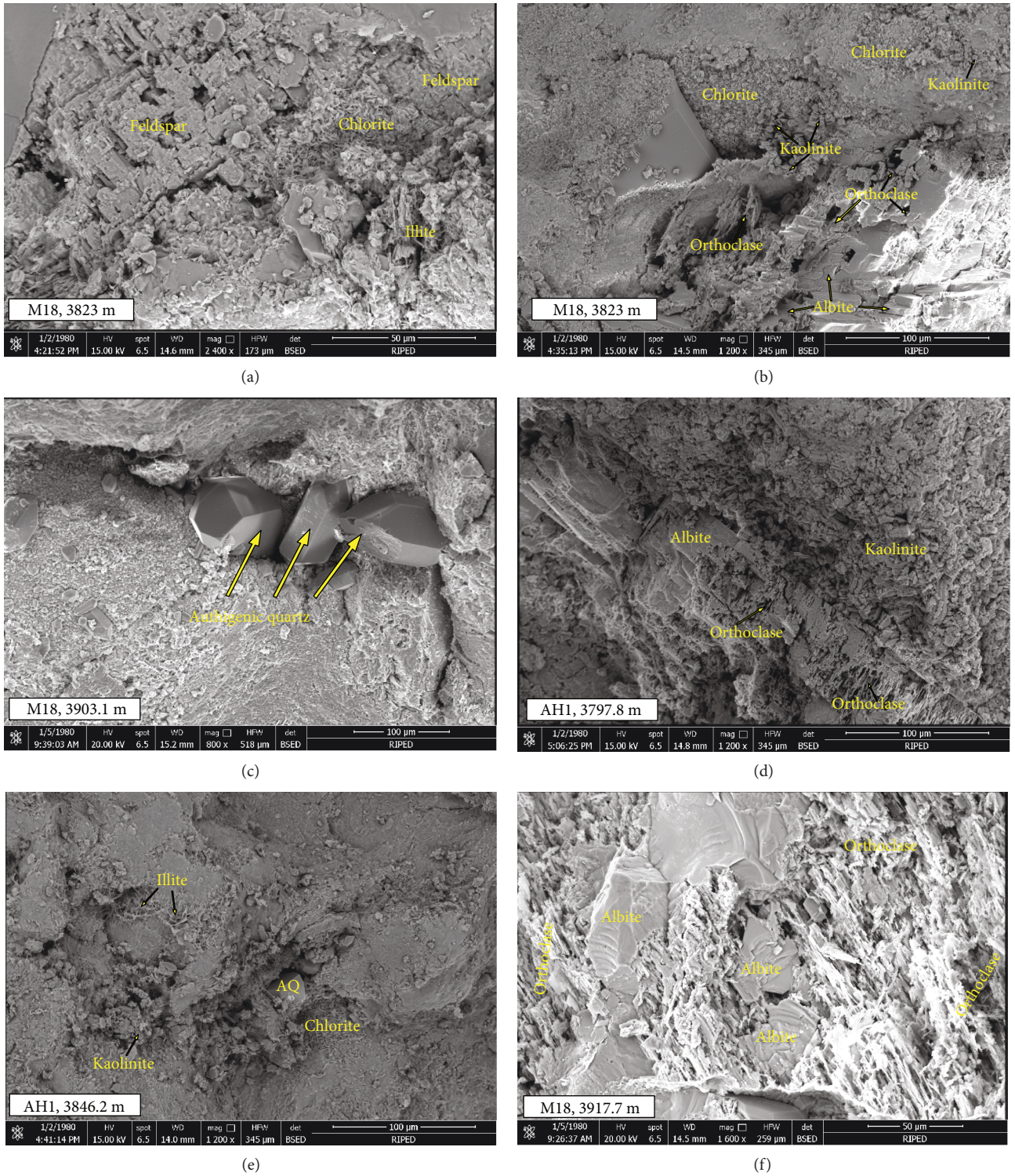

Figure 9: Scanning electron microscope images of the Baikouquan Formation. (a) Leached feldspars, chlorite, and illite; (b) kaolinite and chlorite in primary pores and feldspars; (c) quartz crystals; (d) leached feldspars and kaolinite; (e) clay minerals and quartz crystals; and (f) leached feldspars.

illite and chlorite in alkaline pore water. In the process of K-feldspar dissolution, alkaline ions such as potassium and sodium are constantly generated, the diagenetic system gradually becomes closed, the pore fluid gradually becomes alkaline, and when the temperature reaches 70~100°C, the illitization of feldspars and kaolinite can be expressed as follows [18, 47–49]:

$$3KAlSi_3O_8 + 2H^+ = KAl_3Si_3O_{10}(OH)_2 + 6SiO_2 + 2K^+, \quad (2)$$

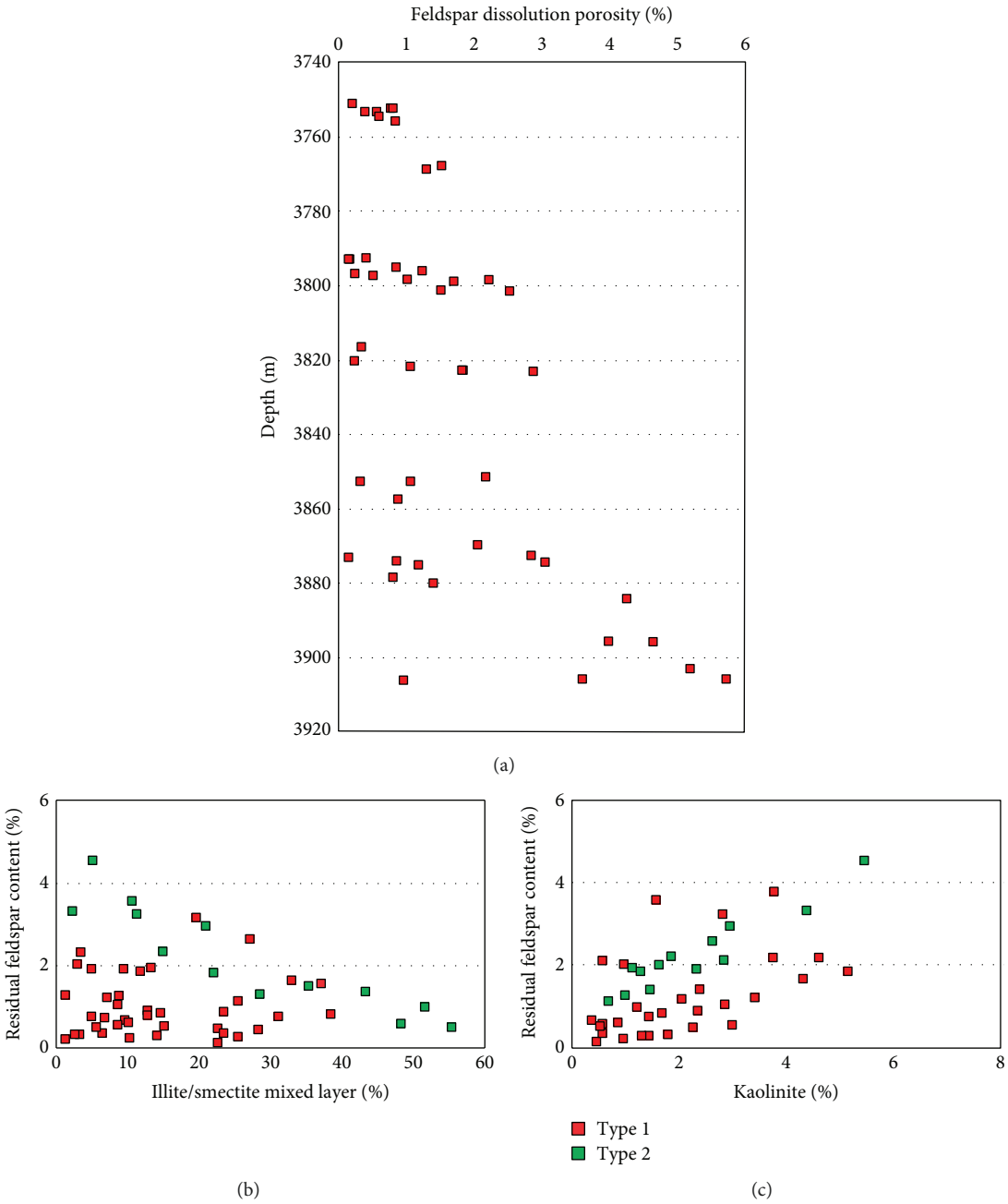

Figure 10: (a) Relationship between the feldspar dissolution and depth; (b) the content of illite-smectite mixed-layer clays and (c) kaolinite; type 1 includes lithofacies of A, B, C, and F in the classification of lithofacies in the study area. Type 2 includes lithofacies of C, E, and G in the classification of lithofacies in the study area.

where $KAl_3Si_3O_{10}(OH)_2$ is illite.

$$Al_2Si_2O_5(OH)_4 + KalSi_3O_8 = KAl_3Si_3O_{10}(OH)_2 + 2SiO_2 + H_2O. \quad (3)$$

Another process that forms illite is montmorillonite illitization, and this process can be expressed as [50]

$$\text{Smectite} + 8Al^{3+} + K^+ = KAl_3Si_3O_{10}(OH)_2 + 3Si^{4+} + Na^+ + 2Ca^{2+} + 2.5Fe^{2+} + 2Mg^{2+}. \quad (4)$$

The minerals on the edge of chlorite are mainly (Figure 11(d)) quartz (27.61%), biotite (22.29%), illite (14.21%), and kaolinite (7.16%). The iron ion released by biotite is the material basis for the transformation of kaolinite into chlorite. When the diagenetic environment changes into a semiclosed system [51] (pH = 9~10) with high amounts of iron and magnesium ions and an appropriate temperature (>90°C) [49], chlorite formation can be described as [52]

$$Al_2Si_2O_5(OH)_4 + 3.5Fe^{2+} + 3.5Mg^{2+} + 9H_2O \rightarrow \text{chlorite} + 14H + . \quad (5)$$

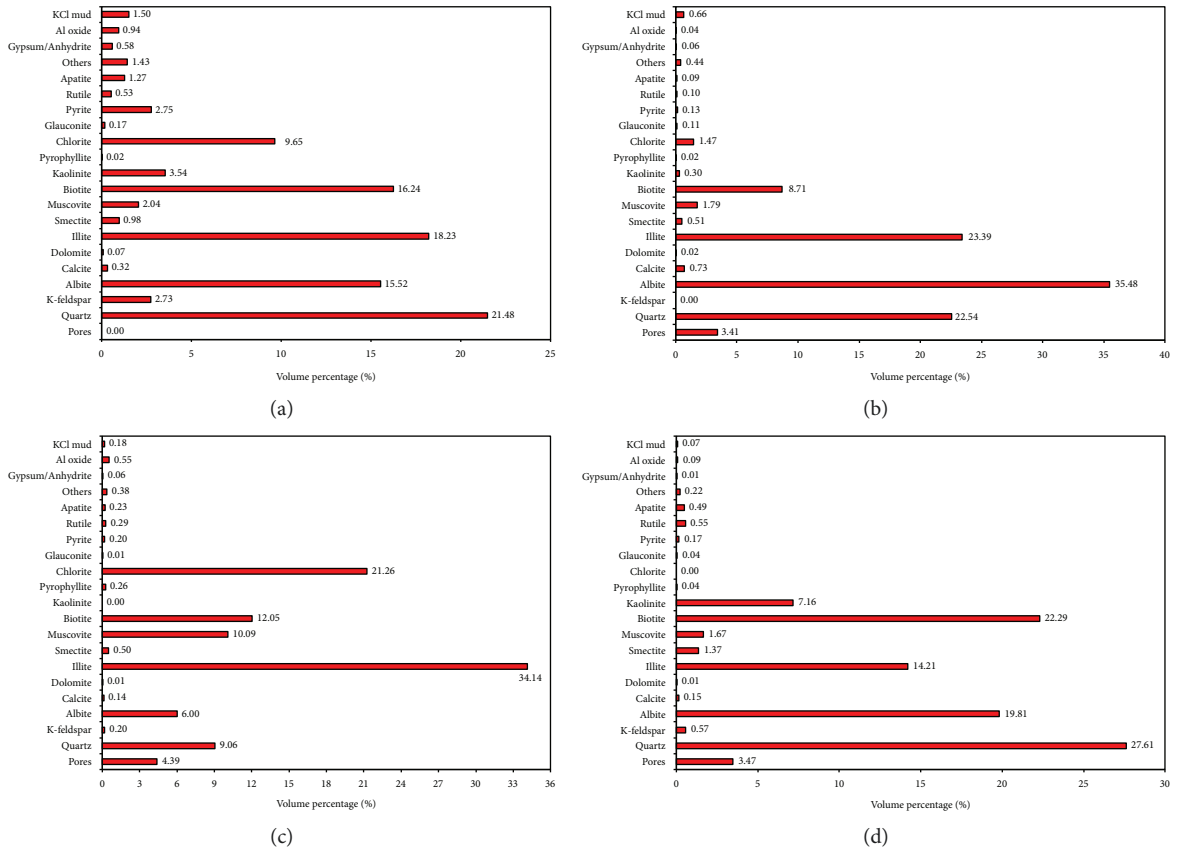

Figure 11: The compositions of paragenetic marginal minerals; (a) pores; (b) K-feldspar; (c) kaolinite, and (d) chlorite.

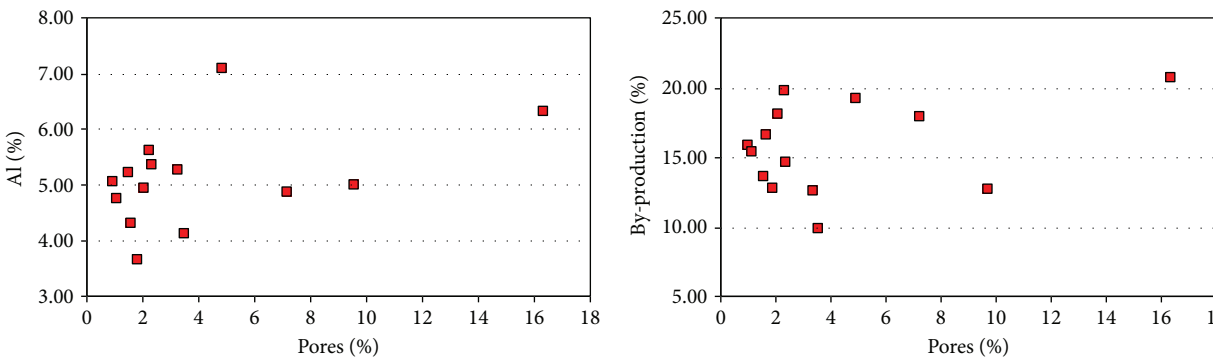

Figure 12: (a) The relationship between the dissolution pores and the aluminium ion and (b) by-product contents.

The feldspar porosity (thin section data) can reach up to 7.12%, but the whole feldspar dissolution by-product is less than 2%; however, in some samples, the by-products can be more than 6%. Based on the formula, feldspar dissolution can provide the large amounts of Al^{3+} and SiO_2 needed for clay mineral and authigenic quartz precipitation [15]. However, the QUEMSCAN analysis shows no positive relationships between the feldspar dissolution pores and the aluminium ion (Figure 12(a)) and dissolution by-products (Figure 12(b)). Thus, we concluded that most of the Al^{3+} and SiO_2(aq) released by feldspar dissolution was moved to a distant area. In a relatively open diagenetic environment, such as the subaqueous distributary channel of a fan delta front (Figure 4(e)), the dissolution by-products are not precipitated in situ [18].

$$KAlSi_3O_8 + 4H^+ = Al^{3+} + 3SiO_2(aq) + K^+ + 2H_2O. \quad (6)$$

The average detrital quartz content in the Baikouquan reservoirs is 44.15%, and the abundant surface area is available for quartz cementation; however, the authigenic quartz content is less than 1%. The fluid inclusion data show that

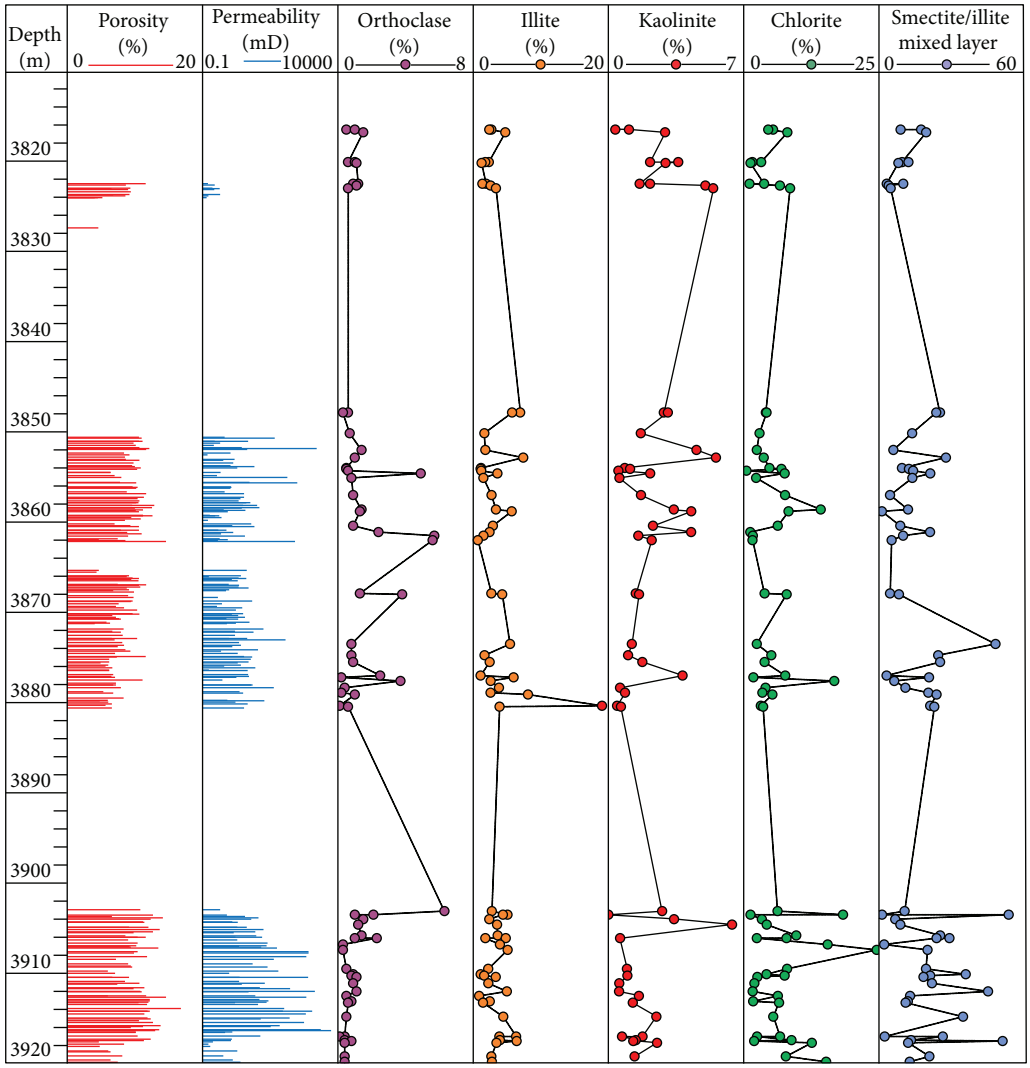

Figure 13: Relationship between the physical properties and clay minerals of the M18 well.

[53] the authigenic quartz precipitated in two phases with temperatures of 70°C–90°C and 100°C–120°C. The illite, smectite, and illite-smectite mixed-layer clay contents are high, and the kaolinite content is relatively low (Figure 13). Smectite consumes many potassium ions when it transforms to illite [54].

5.3. The Impact of Feldspar Dissolution on the Physical Properties of the Reservoir. The K-residual feldspar content is inversely proportional to the porosity (Figures 13 and 14(a)), which indicates that the porosity of the study area is mainly derived from K-feldspar dissolution. The strength of K-feldspar dissolution increases with increasing depth (Figure 10(a)). This is related to the acid flue formed by the hydrocarbon source rocks of the Fengcheng Formation. As the acid moves up through the fault, the dissolution decreases. With increasing K-feldspar dissolution, potassium ions are continuously released, which promotes the transformation of illite-smectite mixed-layer clays to illite, and the illite-smectite mixed-layer clay contents decrease (Figure 10(b)). The kaolinite content significantly increases with the continuous dissolution of K-feldspar (Figure 10(c)).

Observations of thin sections indicate that K-feldspar dissolution in the distributary channel (Figure 4(e)) is more abundant (Figures 6(a), 6(d), and 6(e)) than that in the other sedimentary environments dominated by gravity flow (Figures 6(b) and 6(f)). The lithology of the distributary channel is mainly coarse-grained sandstone, fine-grained conglomerate, and sandy conglomerate. Due to the strong hydrodynamic power of the underwater distributary channel, the mud content is low and the sorting characteristics are good. There is enough space and effective fluid flow conditions to form secondary pores and by-products made by dissolution. The dissolution of feldspar is strong, but the contents of by-products, such as illite and chlorite, are sometimes lower than those (Figures 14(c) and 14(d)) in the braided channel (Figures 4(a) and 4(b)) and the debris flow channel (Figure 4(e)). This indicates that the diagenesis systems in such sedimentary microfacies are more open, the pore water flow velocity is higher, and the dissolution by-products are

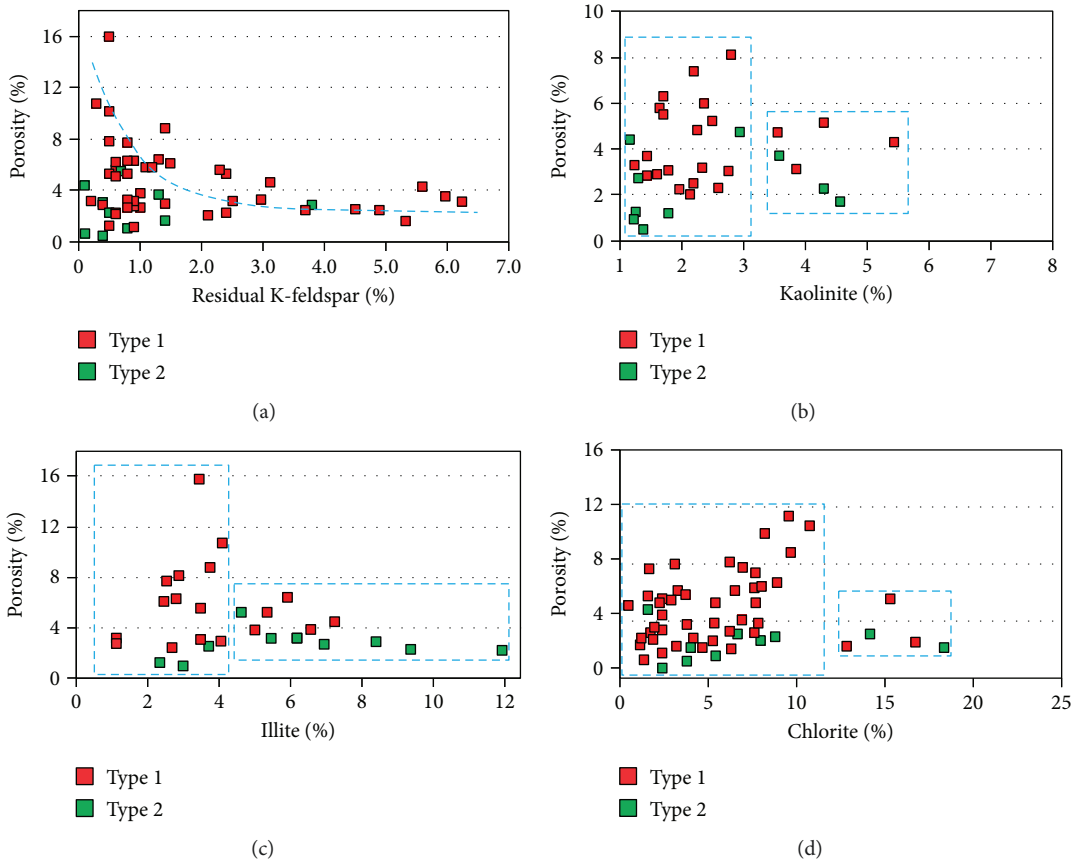

Figure 14: The relationship between porosity and K-feldspar (a), kaolinite (b), illite (c), and chlorite (d); type 1 includes lithofacies of A, B, C, and F in the classification of lithofacies in the study area. Type 2 includes lithofacies of C, E, and G in the classification of lithofacies in the study area.

easily transported, which is beneficial to the increase in porosity and permeability.

In sedimentary microfacies dominated by gravity flow, the intensity of K-feldspar dissolution is weak (less than 1.5%) (Figures 6(b) and 6(f)) and the correlation between the amount of feldspar dissolution and its by-products is good. This shows that the feldspar dissolution products have not been transported at a greater distance but are precipitated at or near the dissolution site, which reflects a relatively closed diagenesis system. Feldspar dissolution in closed systems cannot effectively improve the reservoir properties because the material redistribution is carried out only in the local area [29].

The thin section and XRD data indicate that when the kaolinite content is less than 3%, it is positively correlated with porosity (Figure 14(b)). The intercrystalline pores of kaolinite are favourable for porosity. In a sedimentary environment dominated by gravity flow, the kaolinite content can reach to 4.2%. However, when the kaolinite content is greater than 3%, the porosity is significantly reduced (Figure 14(b)), which indicates that kaolinite occupies a large volume of pores. The average illite content of the study area reservoir is 4.23%, which occurs in reticular and filamentous form and fills the pores, or it occurs as a membrane that wraps around the edges of particles (Figures 9(a) and 9(e)). When the illite content is less than 4%, illite contributes only slightly to the increase in porosity (Figure 14(c)). When the content is greater than 4%, the porosity substantially decreases. Illite can reduce the permeability of the reservoir and affect the reservoir quality [55, 56]. The chlorite film in the study area was formed after the authigenic quartz but before the late calcite cementation (Figure 6(a)), when the reservoir was in its early diagenetic stage B to middle diagenetic stage A. The chlorite content in the subaqueous distributary channel (Figure 4(e)) is high (Figure 6(a)). In a reservoir with high chlorite film content, the contents of illite-smectite mixed-layer clays, illite, and calcite cement are low and the compaction is weak. When the chlorite content is less than 12%, the porosity increases with the increase in chlorite content. When the chlorite content is higher than 12%, the porosity significantly decreases (Figure 14(d)). Because of the precipitation of the chlorite film, the formation of authigenic quartz is inhibited and the compaction, pressure dissolution of quartz, and formation of carbonate cementation decrease, which all have positive impacts on pore preservation [57].

5.4. Feldspar Dissolution and By-Product Distribution Models. Feldspar dissolution is the most important type of dissolution in the Baikouquan Formation of the study area.

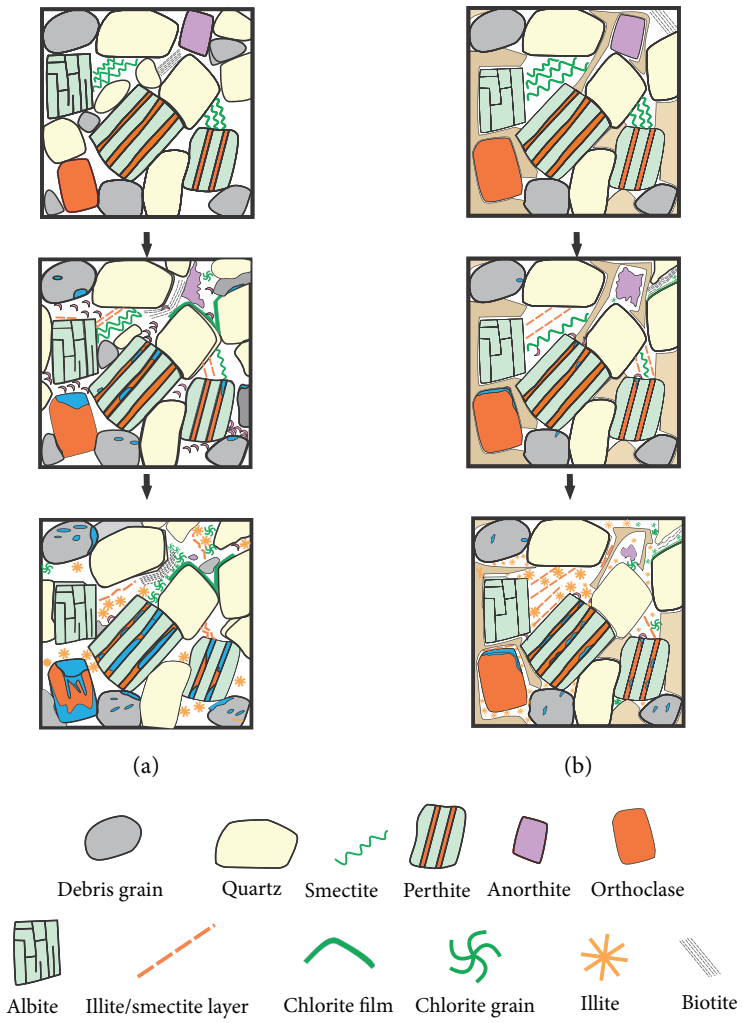

Figure 15: Feldspar dissolution and by-product distribution models; (a) relatively open diagenetic system and (b) relatively closed diagenetic system.

On the basis of the analysis presented above, we can establish the feldspar dissolution and by-product distribution models in different diagenetic systems, which is important to determine the heterogeneity of the reservoir.

Eogenesis took place in the Early Triassic to Early Jurassic at diagenesis temperatures of <85°C [58], and the organic acids at that time were mainly derived from mudstones in the Fengcheng Formation [30]. These fluids flowed through permeable layers and dissolved unstable anorthites [5], which also provided Ca^{2+} for the early-stage low-MnO calcite [59] (Figure 6(c)). Thin section identification and QUEMSCAN analysis indicate that no anorthites exist in these samples. With increasing burial depth, mesogenesis began in the Cretaceous at temperatures ranging from 85°C to 120°C [60]. K-feldspar began to dissolve and formed kaolinite. A large amount of the potassium ions was consumed in the illitization process of smectite, so the two reaction processes promoted each other. At this stage, a large amount of potassium feldspar was dissolved and a large amount of illite/smectite layer clay and kaolinite was formed. Under these diagenetic conditions, Na-feldspar remained stable [61]. The biotite content in the study area is high, which provided Fe^{2+} and Mg^{2+} for the transformation of kaolinite and illite to chlorite.

In relatively open diagenetic systems (Figure 15(a)), such as the underwater distributary channel of the fan delta (Figure 4(e)), the original properties are good, the pore water flows rapidly, and the organic acids from the Fengcheng Formation are easily transported to the reservoir. Because of the relatively open diagenetic system, the by-products formed by K-feldspar dissolution are not deposited in situ (Figure 6(a)) but are carried out by pore water. Therefore, K-feldspar dissolution plays an important role in improving the physical properties of reservoirs in sedimentary environments that are dominated by tractive currents. However, in relatively closed systems (Figures 4(a), 4(c), and 4(f)), the amount of feldspar dissolution is smaller than that in open diagenetic systems (Figure 15(b)). In relatively closed diagenetic systems dominated by gravity flow, the original physical properties are poor and the mud content is high. On the one hand, the acidic fluid needed for dissolution is difficult to transport though a reservoir with poor permeability so the acidic fluid

content required for dissolution is low. On the other hand, the by-products produced by dissolution, such as illite, kaolinite, and chlorite, are difficult to transport in the low-velocity water flow. The concentration of ions in the pore water is saturated so quickly that it is difficult to further dissolve the feldspar. The by-products are basically deposited in situ, for example, chlorite mainly precipitates near illite and biotite. In this diagenetic system, the feldspar dissolution is only redistributed and the physical properties are not significantly increased.

6. Conclusions

(1) The content of feldspar is high in the conglomerate reservoir of the Baikouquan Formation. Feldspar dissolution, mainly K-feldspar dissolution, is the most important diagenetic process in the study area. When the buried depth is 3840–3860 m and 3880–3930 m, the absolute content of secondary pores of feldspar is high and the maximum can reach 6%. With the dissolution of feldspar, the dissolution products of authigenic clay minerals and siliceous cements are precipitated in pores, which have great influence on reservoir quality.

(2) The strength of feldspar dissolution increases with depth but varies in different sedimentary environments. In the subaqueous distributary channel of the subaqueous distributary channel with mainly coarse-grained sandstone and fine-grained conglomerate, the original reservoir properties are good, the mud content is low with good sorting, and there is a relatively large amount of feldspar dissolution. In the lithofacies dominated by gravity flow, the dissolution strength of feldspar is low.

(3) In the subaqueous distributary channel, the content of rigid particles, such as quartz and feldspar, is high and has better sorting and higher original physical properties. In such open diagenetic systems, the velocity of the pore flow is fast and the by-products of the dissolution are easily transported with the fluid and then precipitated in a relatively closed diagenetic system with high mud content and poor original reservoir properties. The strength of dissolution is high, but the by-products of dissolution are relatively less. In the lithofacies dominated by gravity flow, the original physical property is poor and is later easier to become a closed diagenetic system. In this diagenetic system, the acid fluid is difficult to enter the reservoir with poor permeability and the by-products are difficult to be transported. It is also a place where minerals are easily precipitated. In this closed diagenetic system, the dissolution of feldspar has no significant effect on physical properties but only in a smaller range of material redistribution.

(4) The by-products of dissolution are mainly authigenic clay minerals and authigenic quartz. The amount of authigenic quartz in the study area is relatively low, which has few effects on the physical properties of the reservoir. The clay minerals in different diagenetic environments and diagenetic stages have different effects on the reservoir. When the kaolinite content is less than 3%, the illite content is less than 4%, and the chlorite content is less than 12%, the clay minerals have a positive effect on the porosity. The clay minerals can reduce porosity and block the throat when they are larger than these values.

Data Availability

The data used to support the findings of this study are available from the corresponding author upon request.

Conflicts of Interest

The authors declare that they have no conflicts of interest.

Acknowledgments

This work is financially supported by the China National Science and Technology Major Projects (Grant no. 2017ZX05001) and the PetroChina Science and Technology Major Projects (Grant no. 2016B-0304).

References

[1] S. J. Huang, W. H. Wu, J. Liu, L. C. Shen, and C. G. Huang, "Generation of secondary porosity by meteoric water during time of subaerial exposure: an example from Yanchang Formation sandstone of Triassic of Ordos Basin," *Earth Science-Journal of China University of Geosciences*, vol. 4, pp. 419–424, 2003.

[2] M. R. Giles and R. B. De Boer, "Origin and significance of redistributional secondary porosity," *Marine and Petroleum Geology*, vol. 7, no. 4, pp. 378–397, 1990.

[3] R. K. Stoessell and E. D. Pittman, "Secondary porosity revisited: the chemistry of feldspar dissolution by carboxylic acids and anions," *The American Association of Petroleum Geologists Bulletin*, vol. 74, pp. 1795–1805, 1990.

[4] G. Thyne, B. P. Boudreau, M. Ramm, and R. E. Midtbø, "Simulation of potassium feldspar dissolution and illitization in the Statfjord Formation, North Sea," *AAPG Bulletin*, vol. 85, pp. 621–635, 2001.

[5] J. Bevan and D. Savage, "The effect of organic acids on the dissolution of K-feldspar under conditions relevant to burial diagenesis," *Mineralogical Magazine*, vol. 53, no. 372, pp. 415–425, 1989.

[6] R. C. Surdam, S. W. Boese, and L. J. Crossey, "The chemistry of secondary porosity," *AAPG Memoir*, vol. 37, pp. 127–149, 1984.

[7] R. C. Surdam, L. J. Crossey, E. S. Hagen, and S. P. Heasler, "Organic-inorganic and sandstone diagenesis," *AAPG Bulletin*, vol. 73, pp. 1–23, 1989.

[8] J. S. Seewald, "Organic-inorganic interactions in petroleum-producing sedimentary basins," *Nature*, vol. 426, no. 6964, pp. 327–333, 2003.

[9] D. Emery, K. J. Myers, and R. Young, "Ancient subaerial exposure and freshwater leaching in sandstones," *Geology*, vol. 18, no. 12, pp. 1178–1181, 1990.

[10] M. J. Hayes and J. R. Boles, "Volumetric relations between dissolved plagioclase and kaolinite in sandstones: implications for aluminum mass transfer in the San Joaquin Basin, California," *Society for Sedimentary Geology*, vol. 47, pp. 111–123, 1992.

[11] J. H. S. Macquaker, K. G. Taylor, M. Keller, and D. Polya, "Compositional controls on early diagenetic pathways in fine-grained sedimentary rocks: implications for predicting unconventional reservoir attributes of mudstones," *AAPG Bulletin*, vol. 98, no. 3, pp. 587–603, 2014.

[12] S. A. Welch and W. J. Ullman, "Feldspar dissolution in acidic and organic solutions: compositional and pH dependence of dissolution rate," *Geochimica et Cosmochimica Acta*, vol. 60, no. 16, pp. 2939–2948, 1996.

[13] K. Bjørlykke and J. Jahren, "Open or closed geochemical systems during diagenesis in sedimentary basins: constraints on mass transfer during diagenesis and the prediction of porosity in sandstone and carbonate reservoirs," *AAPG Bulletin*, vol. 96, no. 12, pp. 2193–2214, 2012.

[14] I. Parsons, P. Thompson, M. R. Lee, and N. Cayzer, "Alkali feldspar microtextures as provenance indicators in siliciclastic rocks and their role in feldspar dissolution during transport and diagenesis," *Journal of Sedimentary Research*, vol. 75, no. 5, pp. 921–942, 2005.

[15] G. Yuan, Y. Cao, J. Gluyas et al., "Feldspar dissolution, authigenic clays, and quartz cements in open and closed sandstone geochemical systems during diagenesis: typical examples from two sags in Bohai Bay Basin, East China," *AAPG Bulletin*, vol. 99, no. 11, pp. 2121–2154, 2015.

[16] M. Wilkinson, K. L. Milliken, and R. S. Haszeldine, "Systematic destruction of K-feldspar in deeply buried rift and passive margin sandstones," *Journal of the Geological Society*, vol. 158, no. 4, pp. 675–683, 2001.

[17] W. E. Seyfried, D. R. Janecky, and M. E. Berndt, "Rocking autoclaves for hydrothermal experiments II: the flexible reaction cell system," in *Hydrothermal Experimental Techniques*, H. L. Barnes and G. C. Ulmer, Eds., pp. 216–240, Wiley Interscience, 1987.

[18] Q. Fu, P. Lu, H. Konishi et al., "Coupled alkali-feldspar dissolution and secondary mineral precipitation in batch systems: 1. New experiments at 200°C and 300 bars," *Chemical Geology*, vol. 258, no. 3-4, pp. 125–135, 2009.

[19] E. F. McBride, "Quartz cement in sandstones: a review," *Earth-Science Reviews*, vol. 26, no. 1-3, pp. 69–112, 1989.

[20] J. E. Cook, L. B. Goodwin, and D. F. Boutt, "Systematic diagenetic changes in the grain-scale morphology and permeability of a quartz-cemented quartz arenite," *AAPG Bulletin*, vol. 95, no. 6, pp. 1067–1088, 2011.

[21] K. E. Higgs, H. Zwingmann, A. G. Reyes, and R. H. Funnell, "Diagenesis, porosity evolution, and petroleum emplacement in tight gas reservoirs, Taranaki Basin, New Zealand," *Journal of Sedimentary Research*, vol. 77, no. 12, pp. 1003–1025, 2007.

[22] A. Hurst and H. P. Nadeau, "Clay microporosity in reservoir sandstones: an application of quantitative electron microscopy in petrophysical evaluation," *AAPG Bulletin*, vol. 79, pp. 563–573, 1995.

[23] R. E. Grim, "Crystal structures of clay minerals and their X-ray identification," *Earth Science Reviews*, vol. 18, no. 1, pp. 84-85, 1982.

[24] J. S. Jahren and P. Aagaard, "Compositional variations in diagenetic chlorites and illites, and relationships with formation-water chemistry," *Clay Minerals*, vol. 24, no. 2, pp. 157–170, 1989.

[25] M. D. V. Schmidt, "Role of secondary porosity in sandstone diagenesis," *AAPG Bulletin*, vol. 61, pp. 1390-1391, 1977.

[26] S. Zhou, "A study of the secondary pore space in the cretaceous reservoir in the west slope in Songliao Basin," *Petroleum Exploration and Development*, vol. 5, pp. 16–21, 1989.

[27] Y. Chen, C. J. Wang, X. F. Sun, M. Wang, Y. Han, and S. Y. Yan, "Progress on mineral solubility and mechanism of dissolution secondary porosity forming in clastic reservoir," *Bulletin of Mineralogy, Petrology and Geochemistry*, vol. 34, pp. 830–836, 2015.

[28] G. H. Yuan, Y. C. Cao, K. L. Xi, Y. Z. Wang, X. Y. Li, and T. Yang, "Feldspar dissolution and its impact on physical properties of Paleogene clastic reservoir in the northern slope zone of the Dongying Sag," *Acta Petrolei Sinica*, vol. 34, pp. 853–866, 2013.

[29] T. R. Taylor, M. R. Giles, L. A. Hathon et al., "Sandstone diagenesis and reservoir quality prediction: models, myths, and reality," *AAPG Bulletin*, vol. 94, no. 8, pp. 1093–1132, 2010.

[30] X. Kang, W. X. Hu, J. Cao et al., "Selective dissolution of alkali feldspars and its effect on Lower Triassic sandy conglomerate reservoirs in the Junggar Basin, northwestern China," *Geological Journal*, vol. 53, no. 2, pp. 475–499, 2018.

[31] Y. Tang, Y. Xu, J. H. Zhai, X. C. Meng, and Z. W. Zou, "Fan-delta group characteristics and Its distribution of the Triassic Baikouquan reservoirs in Mahu Sag of Junggar Basin," *XinJiang Petroleum Geology*, vol. 35, pp. 628–635, 2014.

[32] F. G. Sui, "Tectonic evolution and its relationship with hydrocarbon accumulation in the northwest margin of Junggar Basin," *Acta Geologica Sinica*, vol. 89, no. 4, pp. 779–793, 2015.

[33] Y. J. Zhang, J. Cao, and W. X. Hu, "Timing of petroleum accumulation and the division of reservoir-forming assemblages, Junggar Basin, NW China," *Petroleum Exploration and Development*, vol. 37, pp. 257–262, 2010.

[34] C. C. Pan, Z. Y. Zhou, S. F. Fan, Q. L. Xie, X. L. Wang, and Y. T. Wang, "Thermal history of Junggar Basin," *Geochimica*, vol. 26, no. 6, pp. 1–7, 1997.

[35] G. Gao, J. Ren, S. Yang, B. Xiang, and W. Zhang, "Characteristics and origin of solid bitumen in glutenites: a case study from the Baikouquan Formation reservoirs of the Mahu Sag in the Junggar Basin, China," *Energy & Fuels*, vol. 31, no. 12, pp. 13179–13189, 2017.

[36] L. J. Huang, Y. Tang, Y. B. Chen et al., "The subfacies boundary description of fan delta under the control of sequence stratigraphy of Triassic Baikouquan formation in the Mahu slope area, Junggar Basin," *Natural Gas Geoscience*, vol. 26, pp. 25–32, 2015.

[37] S. C. Zhang, N. N. Zou, J. A. Shi, Q. S. Chang, X. C. Lu, and B. Chen, "Depositional model of the Triassic Baikouquan Formation in Mabei area of Junggar Basin," *Oil & Gas Geology*, vol. 36, pp. 640–650, 2015.

[38] X. C. Meng, N. G. Chen, H. M. Wang et al., "Sedimentary characteristics of glutenite and its favourable accumulation facies: a case study from T1b, Mabei slope, Junggar Basin," *Acta Sedimentologica Sinica*, vol. 33, pp. 1235–1246, 2015.

[39] X. Li, L. Q. Zhang, H. Shi, and Y. D. Zheng, "Sedimentary environment of Lower Triassic Baikouquan Formation in Mahu Sag, Junggar Basin: a case study from Ma 18 well," *Lithologic reservoirs*, vol. 28, pp. 80–85, 2016.

[40] J. G. Pan, G. D. Wang, Y. Q. Qu et al., "Formation mechanism and characteristic of sandy conglomerate diagenetic trap: a case study of the Triassic Baikouquan Formation in the Mahu Sag, Junggar Basin," *Natural Gas Geoscience*, vol. 26, pp. 41–49, 2015.

[41] L. Van der Plas and A. C. Tobi, "A chart for judging the reliability of point counting results," *American Journal of Science*, vol. 263, no. 1, pp. 87–90, 1965.

[42] X. H. Yu, J. H. Zhai, C. P. Tan, L. Zhang, X. L. Li, and Z. P. Gao, "Conglomerate lithofacies and origin models of fan deltas of Baikouquan Formation in Mahu Sag, Junggar Basin," *XinJiang Petroleum Geology*, vol. 35, no. 6, pp. 619–627, 2014.

[43] C. M. Zhang, X. L. Wng, R. Zhu, J. H. Zhai, J. Pan, and Z. Y. An, "Litho-facies classification of Baikouquan Formation in Mahu Sag, Junggar Basin," *XinJiang Petroleum Geology*, vol. 37, no. 5, pp. 606–614, 2016.

[44] B. Chen, Z. Wang, L. Kang, S. Zhang, and J. Shi, "Diagenesis and pore evolution of Triassic Baikouquan Formation in Mabei region, Junggar Basin," *Journal of Jilin University (Earth Science Edition)*, vol. 46, pp. 23–35, 2016.

[45] J. Jin, X. Kang, W. X. Hu, B. L. Xiang, J. Wang, and J. Cao, "Diagenesis and its influence on coarse clastic reservoirs in the Baikouquan Formation of western slope of the Mahu Depression, Junngar Basin," *Oil & Gas Geology*, vol. 38, pp. 323–333, 2017.

[46] K. Bjørlykke and K. Gran, "Salinity variations in North Sea formation waters: implications for large-scale fluid movements," *Marine and Petroleum Geology*, vol. 11, no. 1, pp. 5–9, 1994.

[47] K. Bjørlykke, "Clay mineral diagenesis in sedimentary basins-a key to the prediction of rock properties, examples from the North Sea Basin," *Clay Minerals*, vol. 33, no. 1, pp. 15–34, 1998.

[48] B. Lanson, D. Beaufort, G. Berger, A. Bauer, A. Cassagnabère, and A. Meunier, "Authigenic kaolin and illitic minerals during burial diagenesis of sandstones: a review," *Clay Minerals*, vol. 37, no. 1, pp. 1–22, 2002.

[49] R. K. Zhu, C. N. Zou, N. Zhang et al., "Diagenetic fluids evolution and genetic mechanism of tight sandstone gas reservoirs in Upper Triassic Xujiahe Formation in Sichuan Basin, China," *Science in China Series D: Earth Sciences*, vol. 51, no. 9, pp. 1340–1353, 2008.

[50] J. Hower, E. V. Eslinger, M. E. Hower, and E. A. Perry, "Mechanism of burial metamorphism of argillaceous sediment: 1. Mineralogical and chemical evidence," *Geological Society of America Bulletin*, vol. 87, no. 5, pp. 725–737, 1976.

[51] H. R. Yuan, Z. Nie, J. Y. Liu, and M. Wang, "Paleogene sedimentary characteristics and their paleoclimatic implications in the Baise Basin, Guangxi," *Acta Geologica Sinica*, vol. 8, pp. 1692–1697, 2007.

[52] Z. Liu, X. F. Tan, J. Wang et al., "Formation mechanism and alteration of clay minerals in clastic rocks—take the Kongdian Fm. of Paleogene in Jiyang depression for example," *Advances in Geosciences*, vol. 5, no. 6, pp. 467–479, 2015.

[53] G. Liu, Z. Chen, X. Wang et al., "Migration and accumulation of crude oils from Permian lacustrine source rocks to Triassic reservoirs in the Mahu Depression of Junggar Basin, NW China: constraints from pyrrolic nitrogen compounds and fluid inclusion analysis," *Organic Geochemistry*, vol. 101, pp. 82–98, 2016.

[54] H. A. Jung, "Transmission and analytical electron microscopy of the smectite-to-illite transition 1," *Clays and Clay Minerals*, vol. 34, no. 2, pp. 165–179, 1986.

[55] M. J. Pearson and J. S. Small, "Illite-smectite diagenesis and palaeotemperatures in Northern North Sea quaternary to Mesozoic shale sequences," *Clay Minerals*, vol. 23, no. 2, pp. 109–132, 1988.

[56] W. R. Xie, W. Yang, X. Y. Zhao et al., "Influences of chlorite on reservoir physical properties of the Xujiahe ormation in the central part of Sichuan Basin," *Petroleum Exploration & Development*, vol. 37, pp. 674–679, 2010.

[57] J. D. Grigsby, "Origin and growth mechanism of authigenic chlorite in sandstones of the lower Vicksburg Formation, South Texas," *Journal of Sedimentary Research*, vol. 71, no. 1, pp. 27–36, 2001.

[58] J. Cao, Y. Zhang, W. Hu et al., "The Permian hybrid petroleum system in the northwest margin of the Junggar Basin, Northwest China," *Marine and Petroleum Geology*, vol. 22, no. 3, pp. 331–349, 2005.

[59] C. V. Jeans, J. G. Mitchell, M. Scherer, and M. J. Fisher, "Origin of the Permo-Triassic clay mica assemblage," *Clay Minerals*, vol. 29, no. 04, pp. 575–589, 1994.

[60] N. S. Qiu, X. L. Wang, H. B. Yang, and Y. Xiang, "The characteristics of temperature distribution in the Junggar Basin," *Chinese Journal of Geology*, vol. 36, pp. 350–358, 2001.

[61] P. Aagaard, P. K. Egeberg, G. C. Saigal, S. Morad, and K. Bjorlykke, "Diagenetic albitization of detrital K-feldspars in Jurassic, Lower Cretaceous and tertiary clastic reservoir rocks from offshore Norway; II, Formation water chemistry and kinetic considerations," *Journal of Sedimentary Research*, vol. 60, no. 4, pp. 575–581, 1990.